AD_____

Award Number: W81XWH-13-1-0165

TITLE: Pluridirectional High-Energy Agile Scanning Electron Radiotherapy (PHASER): Extremely Rapid Treatment for Early Lung Cancer

PRINCIPAL INVESTIGATOR: Peter G Maxim, PhD

CONTRACTING ORGANIZATION: The Leland Stanford Junior University..
Stanford, CA 94305-2004

REPORT DATE: JUNE 2014

TYPE OF REPORT: Annual

PREPARED FOR: U.S. Army Medical Research and Materiel Command
Fort Detrick, Maryland 21702-5012

DISTRIBUTION STATEMENT: Approved for Public Release;
Distribution Unlimited

REPORT DOCUMENTATION PAGE

1. REPORT DATE	2. REPORT TYPE	3. DATES COVERED
June 2014	Annual	15 JUN 2013 – 14 MAY 2014

4. TITLE AND SUBTITLE

Pluridirectional High-Energy Agile Scanning Electron Radiotherapy (PHASER): Extremely Rapid Treatment for Early Lung Cancer

5a. CONTRACT NUMBER

5b. GRANT NUMBER
W81XWH-13-1-0165

5c. PROGRAM ELEMENT NUMBER

6. AUTHOR(S)
Peter G Maxim, PhD,
Billy W Loo, MD, PhD

E-Mail: pmaxim@stanford.edu

5d. PROJECT NUMBER

5e. TASK NUMBER

5f. WORK UNIT NUMBER

7. PERFORMING ORGANIZATION NAME(S) AND ADDRESS(ES)

THE LELAND STANFORD JUNIOR UNIVERSITY

STANFORD, CA 94305-2004

8. PERFORMING ORGANIZATION REPORT NUMBER

9. SPONSORING / MONITORING AGENCY NAME(S) AND ADDRESS(ES)
U.S. Army Medical Research and Materiel Command
Fort Detrick, Maryland 21702-5012

10. SPONSOR/MONITOR'S ACRONYM(S)

11. SPONSOR/MONITOR'S REPORT NUMBER(S)

12. DISTRIBUTION / AVAILABILITY STATEMENT
Approved for Public Release; Distribution Unlimited

13. SUPPLEMENTARY NOTES

14. ABSTRACT We propose to develop a new type of radiotherapy (RT) system for early stage lung cancer using rapidly scanned beams from many directions through electromagnetic steering with no mechanical moving parts, referred to as **pluridirectional high-energy agile scanning electron radiotherapy (PHASER)**. Such a system would be similar in size and cost to commonly available systems, but would deliver an entire treatment of high-dose RT in less than one second, and with even sharper dose sculpting than the current state-of-the-art. In addition, extremely rapid radiation delivery may have a more effective biological impact on tumors for the same radiation dose. We have established a unique multidisciplinary collaboration between Stanford University Department of Radiation Oncology and the Accelerator Research Division at Stanford Linear Accelerator Center (SLAC) National Accelerator Laboratory, to design such a system.

15. SUBJECT TERMS: lung cancer, radiotherapy, biological effectiveness, high energy electrons

16. SECURITY CLASSIFICATION OF:			17. LIMITATION OF ABSTRACT	18. NUMBER OF PAGES	19a. NAME OF RESPONSIBLE PERSON USAMRMC
a. REPORT	**b. ABSTRACT**	**c. THIS PAGE**			**19b. TELEPHONE NUMBER** *(include area code)*
U	U	U	UU	29	

Table of Contents

Contract number: W81XWH-13-1-0165

Title: High-Energy Agile Scanning Electron Radiotherapy (PHASER): Extremely Rapid Treatment for Early Lung Cancer

Principal Investigator: Peter G Maxim, PhD

Introduction:

Cancer is the leading cause of death worldwide and is **increasing epidemically** because of multiple factors including population aging and growth. **Radiation therapy (RT) is a primary curative treatment modality** for cancer whose therapeutic **role and effectiveness are increasing** because of major advances in technology, molecularly targeted drug therapy, and immunotherapy among others. In addition, novel applications of advanced RT for major non-cancer illnesses are rapidly emerging. However, access to RT falls far short of the need for it worldwide and **this gap is growing rapidly**.

We are developing the next generation RT concept, **pluridirectional high-energy agile scanning electron radiotherapy (PHASER)**. The key breakthroughs of the PHASER paradigm are extreme treatment speed that both enables unprecedented accuracy by eliminating the problem of physiologic motion and increases patient throughput; compact and economical design that makes it broadly practical and accessible; improved dose distribution compared to best existing photon therapy based on the use of very high-energy electron (VHEE) beams; and potentially enhanced biological effectiveness. **We envision PHASER as a viable replacement for nearly all existing RT systems, improving clinical effectiveness, cost effectiveness, and availability of curative RT for millions of patients with cancer and other major illnesses in the U.S. and globally.**

We have assembled a research team comprising investigators from the Stanford Department of Radiation Oncology with world-class expertise in clinical radiation oncology, medical physics, and cancer and radiation biology and who have initiated world's first clinical trials of stereotactic ablative radiotherapy for cancer and major pulmonary and cardiovascular diseases, from the Department of Radiology with world-class expertise in imaging system design, and from the SLAC National Accelerator Laboratory with world-class expertise in compact high-energy linear accelerator design, leveraging **talent and resources that can be found nowhere else in the world**.

Our specific aims in this proposal are to produce a practically realizable PHASER design through simulation and experimental validation.

Body:

Task 1 - Specific Aim 1: To determine optimal operating parameters for PHASER using Monte Carlo simulations (months 1-22)

Task 1a: We will perform simulations using an array of MC codes well established in particle physics research: GEANT4, Monte Carlo N-Particle eXtended (MCNPX) and the extension of the Electron Gamma Shower code developed at the National Research Council Canada (EGSnrc). This will permit cross validation of codes and also simulation of electronuclear and photonuclear interactions not available in all of the codes (months 1-5).

Task 1b: Clinical scenarios: We will simulate treatment of 4 different body regions with varying tissue characteristics – head/neck, thorax (lung), abdomen (liver), and pelvis (prostate) – using representative CT data sets for each site. In each site, we will simulate both focal and extended (locally advanced) tumor targets (months 5-12).

Task 1c: Treatment planning and plan evaluation: PHASER plans will be manually optimized by forward planning. They will be compared with the best achievable photon VMAT plans in each case. Comparisons will be made by normalizing all plans to achieve the same volumetric coverage (95%) of the planning target volume (PTV) by the prescription dose, and comparing the conformity index at various isodose levels, defined as the ratio of the respective isodose volume to the PTV. In addition, we will code a treatment plan optimizer in MATLAB based on published literature (month 13-17).

Task 1d: Treatment planning optimization: We will develop an in-house inverse treatment planning optimization system based on simulated annealing and Monte Carlo simulations. We will use the optimization schemes for comparison of optimized PHASER treatment plans to state-of-the-art photon VMAT plans. We will also investigate the impact of variables such as body habitus and implanted prostheses.

Status Specific Aim 1:

We have analyzed the three MC codes and found excellent agreement between MCNPX and EGSnrc. The latest version of GEANT4 shows significant deviations (7% for a 5x5cm and 5% for 1x1 cm 100 MeV) from EGSnrc and MCNPX. Here, we have calculated percent depth doses in water phantoms and noted a 7% deviation for a 5x5 cm field size and a deviation of 5% for a 1x1cm field size. We will investigate the reason for this deviation form the other two codes.

We have developed a software interface to allow high-accuracy Monte Carlo simulations of VHEE dose calculations to be set up and imported into an advanced commercial treatment planning system (provided by RaySearch Laboratories, through an established research collaboration) which allows complete inverse planning optimization. This allows us to produce treatment plans as though PHASER were clinically available, and compare these treatment plans with the best current photon-based plans. We have now simulated treatments of a broad range of anatomic sites, including head and neck, lung, liver, pelvis (with and without metallic prosthetic implants), and pediatric brain, including both small and extended field targets (Figure 1).

These simulations demonstrate that for diverse clinical scenarios, VHEE in the practically achievable energy range of 80-100 MeV consistently produces equal or superior dose distributions compared with the best clinically used photon VMAT plans.
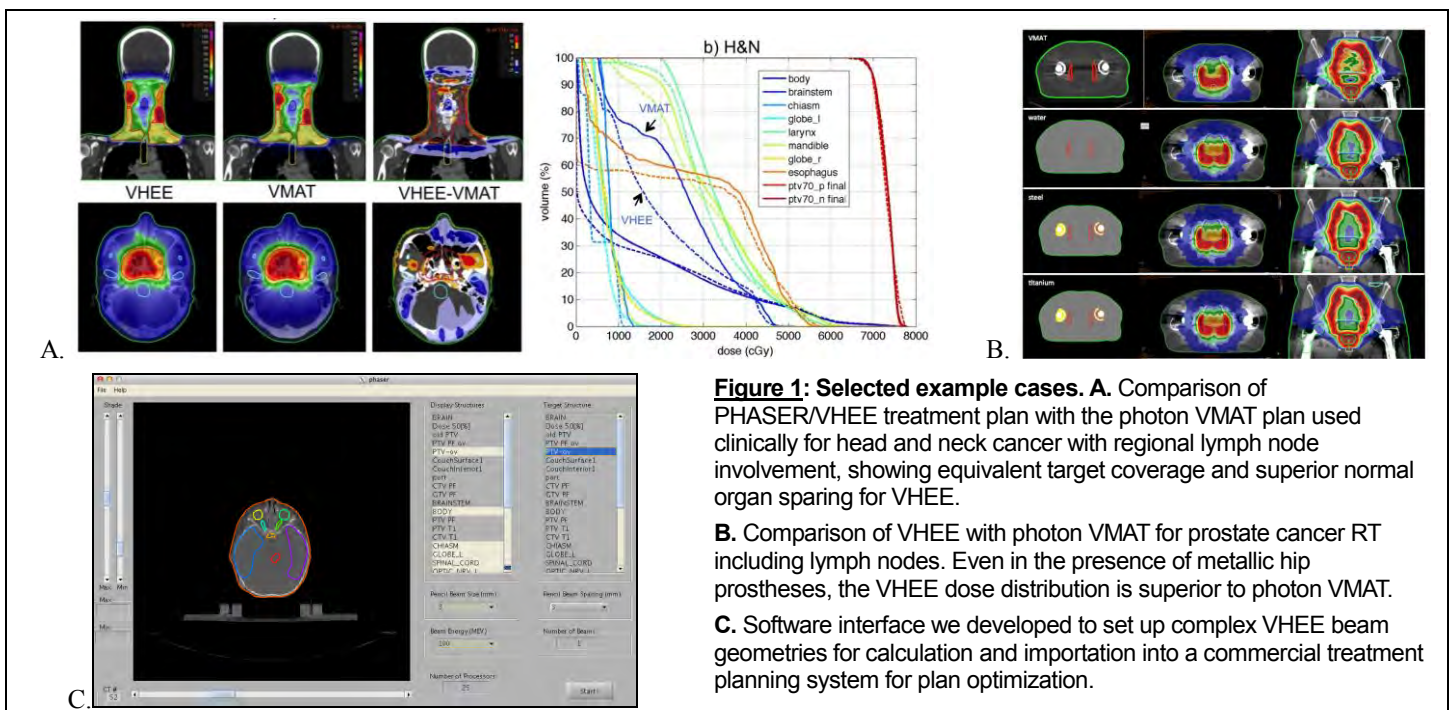
Figure 1: Selected example cases. A. Comparison of PHASER/VHEE treatment plan with the photon VMAT plan used clinically for head and neck cancer with regional lymph node involvement, showing equivalent target coverage and superior normal organ sparing for VHEE.

B. Comparison of VHEE with photon VMAT for prostate cancer RT including lymph nodes. Even in the presence of metallic hip prostheses, the VHEE dose distribution is superior to photon VMAT.

C. Software interface we developed to set up complex VHEE beam geometries for calculation and importation into a commercial treatment planning system for plan optimization.

This work has now been submitted and **selected for two oral presentations (one as a Featured Presentation) and a poster at the upcoming 2014 American Association for Physicists in Medicine (AAPM) meeting**. Work is now ongoing to optimize systematically the most critical operating parameters of beam number and geometry and beam energy including variable beam energy within the same plan for the various clinical scenarios.

Task 2 - Specific Aim 2: To perform experimental validation and calibration of the Monte Carlo codes at NLCTA (SLAC) (months 10-22)

Task 2a: Homogeneous phantom measurements: As described in our preliminary results above, we have constructed a homogeneous phantom using slabs of tissue equivalent polystyrene plastic, between which films can be inserted to record the dose profiles. We will measure beam profiles for field sizes ranging from 0.1-5 cm and electron energies ranging from 50-100 MeV (months 8-15).

Task 2b Heterogeneous phantom measurements: We will construct a series of heterogeneous phantoms consisting of slabs of polystyrene stacking to form a 15 cm cube, with features of various densities inserted to simulate different tissue types (months 15-22).

Status Specific Aim 2:

We have completed Task2a and submitted a manuscript to the 'International Journal of Radiation Oncology, Biology and Physics' (Red Journal) detailing our results of homogenous phantom measurements. The submitted manuscript is attached to this report.

We have already begun the heterogeneous phantom and anticipate finalizing the measurements and analysis by the end of month 22.

Task 3: Data analysis and submission for publication in peer reviewed journal (months 23-24).

Key Research Accomplishments:

- We have developed a software interface for Monte Carlo calculations.
- We have established a research collaboration with RaySearch Laboratories that includes a license for their commercially available treatment planning system, which allows inverse planning optimization.
- We have demonstrated proof of principle that 80-100 MeV electrons consistently produce equal or superior dose distributions compared with the best clinically used photon VMAT plans.
- We have completed the proposed homogenous phantom measurements and submitted a manuscript to the Red Journal (please see attachment).

Reportable Outcomes:

The following abstracts have been selected for oral/poster presentation at the 56th Annual

Meeting of the American Association of Physicists in Medicine (AAPM):

1) FEATURED PRESENTATION - Treatment Planning Tool for Radiotherapy with Very High-Energy Electron Beams

M Bazalova[1]*, B Qu[1] , E Hynning[2] , B Hardemark[2] , B Palma[1] , B Loo[1] , P Maxim[1] , (1) Stanford University, Stanford, CA, (2) RaySearch Laboratories, Stockholm, Sweden

Purpose: To develop a tool for treatment planning optimization for fast radiotherapy delivered with very high-energy electron beams (VHEE) and to compare VHEE plans to state-of-the-art plans for challenging pelvis and H&N cases.

Methods: Treatment planning for radiotherapy delivered with VHEE scanning pencil beams was performed by integrating EGSnrc Monte Carlo (MC) dose calculations with spot scanning optimization run in a research version of RayStation. A Matlab GUI for MC beamlet generation was developed, in which treatment parameters such as the pencil beam size and spacing, energy and number of beams can be selected. Treatment planning study for H&N and pelvis cases was performed and the effect of treatment parameters on the delivered dose distributions was evaluated and compared to the clinical treatment plans. The pelvis case with a 691cm3 PTV was treated with 2-arc 15MV VMAT and the H&N case with four PTVs with total volume of 531cm3 was treated with 4-arc 6MV VMAT.

Results: Most studied VHEE plans outperformed VMAT plans. The best pelvis 80MeV VHEE plan with 25 beams resulted in 12% body dose sparing and 8% sparing to the bowel and right femur compared to the VMAT plan. The 100MeV plan was superior to the 150MeV plan. Mixing 100 and 150MeV improved dose sparing to the bladder by 7% compared to either plan. Plans with 16 and 36 beams did not significantly affect the dose distributions compared to 25 beam plans. The best H&N 100MeV VHEE plan decreased mean doses to the brainstem, chiasm, and both globes by 10-42% compared to the VMAT plan.

Conclusion: The pelvis and H&N cases suggested that sixteen 100MeV beams might be sufficient specifications of a novel VHEE treatment machine. However, optimum machine parameters will be determined with the presented VHEE treatment-planning tool for a large number of clinical cases.

2) The Effect of Beam Parameters On Very High-Energy Electron Radiotherapy: A Planning Study

B Palma[1]*, M Bazalova[1] , B Hardemark[2] , E Hynning[2] , B Qu[1] , B Loo[1] , P Maxim[1] , (1)Department of Radiation Oncology, Stanford University, Stanford, CA, (2) RaySearch Laboratories AB, Stockholm, Sweden

Purpose: We evaluated the effect of very high-energy electron (VHEE) beam parameters on the planning of a lung cancer case by means of Monte Carlo simulations.

Methods: We simulated VHEE radiotherapy plans using the EGSnrc/BEAMnrc-DOSXYZnrc code. We selected a lung cancer case that was treated with 6MV photon VMAT to be planned with VHEE. We studied the effect of beam energy (80 MeV, 100 MeV, and 120 MeV), number of equidistant beams (16 or 32), and beamlets sizes (3 mm, 5 mm or 7 mm) on PTV coverage, sparing of organs at risk (OARs) and dose conformity. Inverse-planning optimization was performed in a research version of RayStation (RaySearch Laboratories AB) using identical objective functions and constraints for all VHEE plans.

Results: Similar PTV coverage and dose conformity was achieved by all the VHEE plans. The 100 MeV and 120 MeV VHEE plans were equivalent amongst them and were superior to the 80 MeV plan in terms of OARs sparing. The effect of using 16 or 32 equidistant beams was a mean difference in average dose of 2.4% (0%-7.7%) between the two plans. The use of 3 mm beamlet size systematically reduced the dose to all the OARs. Based on these results we selected the 100MeV-16beams-3mm-beamlet-size plan to compare it against VMAT. The selected VHEE plan was more conformal than VMAT and improved OAR sparing (heart and trachea received 125% and 177% lower dose, respectively) especially in the low-dose region.

Conclusion: We determined the VHEE beam parameters that maximized the OAR dose sparing and dose conformity of the actually delivered VMAT plan of a lung cancer case. The selected parameters could be used for the planning of other treatment sites with similar size, shape, and location. For larger targets, a larger beamlet size might be used without significantly increasing the dose.

3) Radiation Therapy with Very High-Energy Electron (VHEE) Beams in the Presence of Metal Implants (Poster presentation)

C Jensen[1]*, B Palma[1], B Qu[1], P Maxim[1], B Hardemark [2], E Hynning [2], B Loo[1], M Bazalova[1], (1)Department of Radiation Oncology, Stanford University, Stanford, CA, (2) RaySearch Laboratories, Stockholm, Sweden

Purpose: To evaluate the effect of metal implants on treatment plans for radiation therapy with very high-energy electron (VHEE) beams.

Methods: The DOSXYZnrc/BEAMnrc Monte Carlo (MC) codes were used to simulate 50-150MeV VHEE beam dose deposition and its effects on steel and titanium (Ti) heterogeneities in a water phantom. Heterogeneities of thicknesses ranging from 0.5cm to 2cm were placed at 10cm depth. MC was also used to calculate electron and photon spectra generated by the VHEE beams' interaction with metal heterogeneities. The original VMAT patient dose calculation was planned in Eclipse. Patient dose calculations with MC-generated beamlets were planned using a Matlab GUI and research version of RayStation. VHEE MC treatment planning was performed on water-only geometry and water with segmented prostheses (steel and Ti) geometries with 100MeV and 150MeV beams.

Results: 100MeV PDD 5cm behind steel/Ti heterogeneity was 51% less than in the water-only phantom. For some cases, dose enhancement lateral to the borders of the phantom increased the dose by up to 22% in steel and 18% in Ti heterogeneities. The dose immediately behind steel heterogeneity decreased by an average of 6%, although for 150MeV, the steel heterogeneity created a 23% increase in dose directly behind it. The average dose immediately behind Ti heterogeneities increased 10%. The prostate VHEE plans resulted in mean dose decrease to the bowel (20%), bladder (7%), and the urethra (5%) compared to the 15MV VMAT plan. The average dose to the body with prosthetic implants was 5% higher than to the body without implants.

Conclusion: Based on MC simulations, metallic implants introduce dose perturbations to VHEE beams from lateral scatter and backscatter. However, when performing clinical planning on a prostate case, the use of multiple beams and inverse planning still produces VHEE plans that are dosimetrically superior to photon VMAT plans.

Conclusion:

We have made significant progress towards the proposed project. We have demonstrated that the computational tools (Monte Carlo codes) are adequate to simulate the interaction of VHEE in tissue and phantoms. We have also demonstrated proof of principle that for diverse clinical scenarios, VHEE in the practically achievable energy range of 80-100 MeV consistently produces equal or superior dose distributions compared with the best clinically used photon VMAT plans.

References

No references to cite.

Appendices:

TITLE: Comparison of film measurements and Monte Carlo simulations of dose delivered with very high-energy electron beams in a homogeneous phantom

RUNNING TITLE: Measurements and MC simulations of VHEE beams

AUTHORS: Magdalena Bazalova, Ph.D.[1], Michael Liu, M.Sc.[1], Michael Dunning, Ph.D.[2], Doug McCormick[2], Janice Nelson[2], Keith Jobe[2], Eric Colby, Ph.D.[2, 3], Albert C. Koong, M.D. PhD.[1], Sami Tantawi, Ph.D.[2], Valery Dolgashev, Ph.D.[2], *Peter G. Maxim, Ph.D.[1], and *Billy W. Loo Jr., M.D. Ph.D.[1]

1-Department of Radiation Oncology, Stanford University, Stanford, CA
2-SLAC National Accelerator Laboratory, Menlo Park, CA
3-Now at U.S. Department of Energy, Washington, DC

*CO-CORRESPONDING AUTHORS

Billy W. Loo Jr., M.D. Ph.D.
Department of Radiation Oncology and Stanford Cancer Institute
Stanford University School of Medicine
875 Blake Wilbur Drive
Stanford, CA 94305-5847
E-mail: BWLoo@Stanford.edu

AND

Peter G. Maxim, Ph.D.
Department of Radiation Oncology and Stanford Cancer Institute
Stanford University School of Medicine
875 Blake Wilbur Drive
Stanford, CA 94305-5847
E-mail: Peter.Maxim@Stanford.edu

KEY WORDS

Monte Carlo, dose calculations, very high-energy electrons

SUBMITTED TO: International Journal of Radiation Oncology, Biology, Physics

DISCLOSURES

TITLE: Comparison of film measurements and Monte Carlo simulations of dose delivered with very high-energy electron beams in a homogeneous phantom

RUNNING TITLE: Measurements and MC simulations of VHEE beams

SUMMARY (Word limit: 75)

We have performed measurements of dose deposition for very high-energy electron beams of 50-70 MeV in a homogeneous phantom and compared them to Monte Carlo simulations. We have demonstrated agreement in relative dose within 5% for pencil beam sizes of approximately 4-7 mm. Our study represents an important step towards treatment planning for rapid radiotherapy with very-high energy electron beams.

ABSTRACT (Word count limit: 300)

Purpose/Objective: Very high-energy electron (VHEE) beams have promising characteristics for radiation therapy. Our goal was to measure dose distributions of VHEE beams in a homogeneous phantom on an experimental beamline and compare the results with Monte Carlo (MC) modeling.

Methods and Materials: Dose in a polystyrene phantom delivered by an experimental VHEE beam line was measured with EBT2 Gafchromic films for 50 MeV and 70 MeV beams of 3.95-6.93 mm diameter and compared to corresponding MC-simulated dose distributions. MC dose in the polystyrene phantom was calculated with the EGSnrc/BEAMnrc and DOSXYZnrc codes based on the experimental setup. Additionally, the effect of 2% beam energy measurement uncertainty and possible non-zero beam angular spread on MC dose distributions was evaluated.

Results: MC simulated percentage depth dose (PDD) curves agreed to measurements within 4% for all beam sizes for both 50 MeV and 70 MeV VHEE beams. Central axis PDD at 8 cm depth ranged from 14% to 19% for the 5.44-6.93 mm 50 MeV beams and it ranged from 14% to 24% for the 3.95-5.74 mm 70 MeV beams. MC simulated relative beam profiles evaluated at depths of 0.64 to 7.46 cm agreed to measurements within 5%. The 2% beam energy uncertainty and 0.286° beam angular spread correspond to a 3.0% and 3.8% difference in depth dose curves of the 50 and 70 MeV electron beams, respectively.

Conclusions: We have demonstrated that dose distributions for VHEE beams can be measured with EBT2 Gafchromic films and modeled with Monte Carlo. The model will facilitate dose calculations for radiobiological experiments as well as for potential radiation therapy using VHEE beams.

MANUSCRIPT (Word count limit: [3500])

1. Introduction

External beam radiation therapy has been historically most frequently delivered with medical linear accelerators generating photon and electron beams with energies in the range between 5 and 20 MeV. Megavoltage (MV) photon beams of these energies have suitable attenuation and dose deposition properties for treatments of deep-seated tumors (1). Electron beams of similar energy, however, deposit a large fraction of their energy on the skin and are mostly used for treatments of superficial cancers (2, 3).

Previous work has demonstrated in principle a number of advantages of using very high-energy (50-250 MeV) electron (VHEE) beams for radiation therapy of deep-seated tumors (4-7). Monte Carlo (MC) simulations with the PENELOPE (8, 9) code showed that electron beams of such high energies have similar to superior dose deposition properties compared to currently clinically used photon beams. For example, intensity-modulated VHEE therapy for prostate cancer at 250 MeV energy outperformed intensity-modulated radiation therapy (IMRT) with 15 MV photon beams (7).

The dosimetric advantages of VHEE stem from favorable depth-dose characteristics relative to photons, with a flatter initial profile to clinically relevant depths followed by a more rapid falloff with a range that depends on the beam energy, as well as minimal loss of electronic equilibrium at interfaces between media of different density, resulting in much less sensitivity to tissue heterogeneity (4). Thus when multiple beams are used, higher conformity and lower integral dose for the same target coverage is possible with VHEE compared to photons, intermediate between photons and protons, and with less concern about underdosing in buildup regions or range uncertainty issues.

Monte Carlo (MC) simulation is the core methodology for dose calculation of VHEE for potential radiation therapy applications. To date however, there has been minimal comparison of Monte Carlo codes to experimental data for electrons in the 50-100 MeV energy range in tissue equivalent materials, due mainly to lack of availability of VHEE beams experimentally (4). Experimental dose measurements and MC dose calculations with the DPM code up to 50 MeV from the racetrack microtron have been published (10-12). In this work, we present experimental measurements of dose deposition of 50 and 70 MeV VHEE beams in a homogeneous phantom acquired at an experimental beam line and compared them to EGSnrc (13) MC simulations.

2. Materials and Methods

2.1. Experimental measurements on a VHEE beam line

Measurements of VHEE beam percentage depth-dose curves (PDDs) and dose profiles were performed at the Next Linear Collider Test Accelerator (NLCTA) located at [BLINDED] (14). The electron beam is produced by an S-band RF photoinjector, is further accelerated by two high-gradient X-band RF accelerating structures, and is transported approximately 25 meters to the experimental station inside a beam line with aperture varying from 6-20 mm. There are several quadrupole and dipole magnets to assist in beam transport, and diagnostics to monitor beam energy, energy spread, charge, beam size, and beam position. The NCLTA beam line was modified to accommodate the experimental setup. A 50-μm thick vacuum window of 1.27 cm in diameter made of stainless steel was used to interface the beam line with open air, in which a dose phantom was placed. Dose distributions of 50 MeV and 70 MeV beams were measured using radiochromic films that were embedded in the polystyrene phantom (Figure 1a,b). The beam energy was monitored using a large electro-magnet and a phosphorescent screen. Two thin scintillator screens placed in the front and behind the phantom were used to monitor the beam size that was controlled with magnets located upstream from the exit window. The scintillator

screens were moved out of the beam line when the phantom was irradiated. The various beam sizes and shapes measured by the first film are shown in Figure 1c.

The dose phantom consisted of stacked polystyrene $(C_8H_8)_n$ slabs with mass density of 1.05 g/cm^3, which is comparable to water. Sheets of Gafchromic EBT2 dosimetry film (ISP, Wayne,
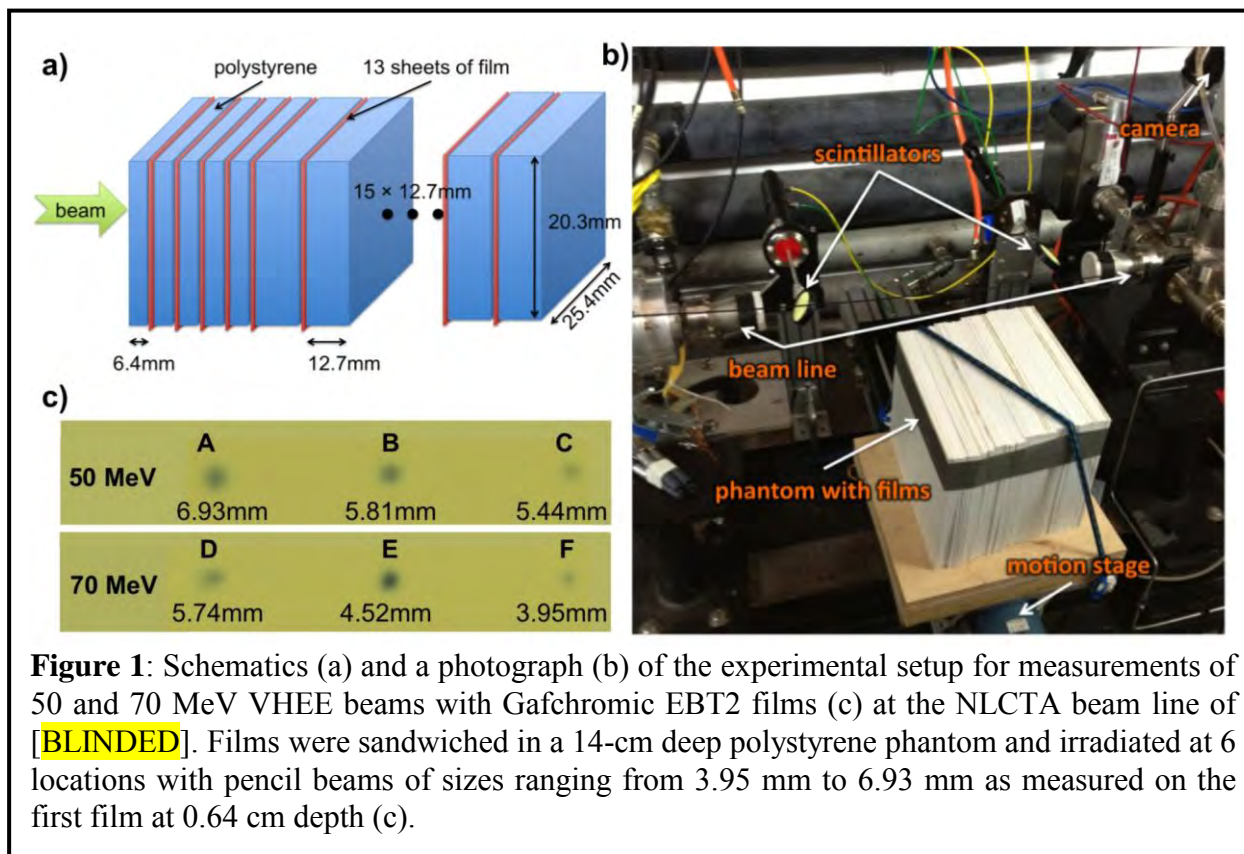
Figure 1: Schematics (a) and a photograph (b) of the experimental setup for measurements of 50 and 70 MeV VHEE beams with Gafchromic EBT2 films (c) at the NLCTA beam line of [BLINDED]. Films were sandwiched in a 14-cm deep polystyrene phantom and irradiated at 6 locations with pencil beams of sizes ranging from 3.95 mm to 6.93 mm as measured on the first film at 0.64 cm depth (c).

NJ) were placed at 13 depths ranging from 6.4 mm to 12.7 cm. The phantom was placed 15 cm away from the beam line exit window.

Magnets upstream of the steel exit window were used to alter the beam size allowing for three beam sizes at each of the two energies. Nominally, the beam sizes were chosen to be 5, 3, and 2 mm for the 50 MeV beam and 5, 2, and 1 mm for the 70 MeV beam. However, accurate adjustment of the beam size was not possible with the existing beam diagnostics equipment. The number of pulses was altered based on MC simulations to approximately achieve similar doses at the films, with 40, 20, and 10 pulses at 50 MeV and 40, 20, and 3 pulses at 70 MeV. The charge

per each pulse was 30 pC resulting in ~1.87×10^8 electrons/pulse. Each pulse was 1 ps long and pulses were delivered with 1 Hz repetition rate. Due to the imperfect focusing and subsequent blurring of the beam and beam divergence caused by the exit window and air between the window and the phantom, the film-measured beam sizes were larger than the beam sizes observed on the scintillator screens. The beam parameters as well as beam sizes on the first film placed at 0.64 cm depth and at the exit window are summarized in Table 1.

The irradiated Gafchromic EBT2 films were digitized on a Perfection V500 flatbed scanner (EPSON, Long Beach, CA) with 254-dpi resolution. The film was calibrated using a 12 MeV electron beam generated by a clinical linear accelerator.

2.2. Monte Carlo modeling of VHEE experiment

The EGSnrc BEAMnrc/DOSXYZnrc MC codes were selected to model the experimental setup (15, 16). The steel window and the polystyrene phantom were included in the simulations. According to the NLCTA beam specifications, 2D incident Gaussian beams with no beam angular beam spread were first assumed. Electron pencil beams passing through the steel window were simulated in the BEAMnrc code and dose deposition in phantoms was simulated with the BEAMnrc-generated phase-space file in the DOSXYZnrc code. According to the experimental setup, the window to phantom distance was set to 15 cm. A voxel size of $0.5 \times 0.5 \times 0.5$ mm^3 was used for dose scoring and the number of primary electrons used for each simulation was set to 1×10^7. All interactions, including triplet production, photonuclear attenuation, radiative Compton correction, electron impact ionization, and Rayleigh scattering were included in the simulations. Electrons and photons were tracked down to 10 keV. The measured and calculated dose distributions were compared by means of PDD curves and beam profiles at four depths using Matlab (The Mathworks, Natick, MA).

2.3. Monte Carlo modeling of beam angular spread

The presence of the steel window in the beam line caused an angular spread of the low-emittance input electron beam. Since the dimensions of the input electron beam could not be measured accurately, the angular spread was investigated by simulating a range of input Gaussian beam widths and calculating the expected beam profile at the location of the first film at 0.64 cm depth in the phantom positioned 15 cm from the exit window. From this relationship, the experimental input beam widths were back-calculated from the film measurements based on a second order polynomial fit applied to the data.

The effects of angular beam spread and VHEE beam energy distribution on the measured dose distribution were also investigated by means of MC simulations. Specifically, central-axis depth dose of the largest beam sizes for both beam energies were simulated with the maximum possible energy spread and angular beam spread. The maximum possible angular beam spread of 0.286° was estimated from the 60 cm distance between the first upstream electromagnet to the exit window and the 6 mm FWHM beam that passes through the exit window without being clipped. Due to the energy measurement accuracy of 2%, dose distributions for 50.0±1.0 MeV and 70.0±1.4 MeV were simulated. Similarly, the effect of the 0.25% FWHM energy spread on dose distributions of the largest beams was studied.

2.4. Monte Carlo modeling of x-ray contamination due to the exit window

The amount of x-ray production in the steel exit window was determined. Electron beams with 50 and 70 MeV of 2-mm FWHM interacted with the 50-µm thick steel window and phase-space files downstream of the steel window were scored. Central-axis PDD in a water phantom calculated only with x-rays generated in the exit window was compared to the central-axis PDD calculated with all particles in the phase-space file.

2.5. Monte Carlo modeling of film energy response

Energy response of Gafchromic EBT2 films to electrons was shown to be flat for electron energies between 6-20 MeV (17). Since no data was available for energy response of the films to VHEE beams, we used MC simulations to predict the energy response of VHEE based on the work presented by Sutherland et *al* (18). Monoenergetic beams of 1-100 MeV and 1-cm in size interacted with a sheet of Gafchromic EBT2 film placed on a 10 cm polystyrene phantom. The dose to the film D_{EBT2} was quantified by simulating the dose deposited in the film active layer. In order to evaluate the film energy response by means of D_{EBT2}/D_{water}, the dose with identical simulation setup but with the film material replaced with water D_{water} was modeled.

We would like to note that beam pulse length of 1 ps resulted in maximum dose rates of 3.6×10^{11} Gy/s. It has been demonstrated that Gafchromic EBT films were dose rate independent for irradiations with 20 MeV beams up to 1.5×10^{10} Gy/s (19). Here we assumed that Gafchromic EBT2 films are dose rate independent up to 3.6×10^{11} Gy/s.
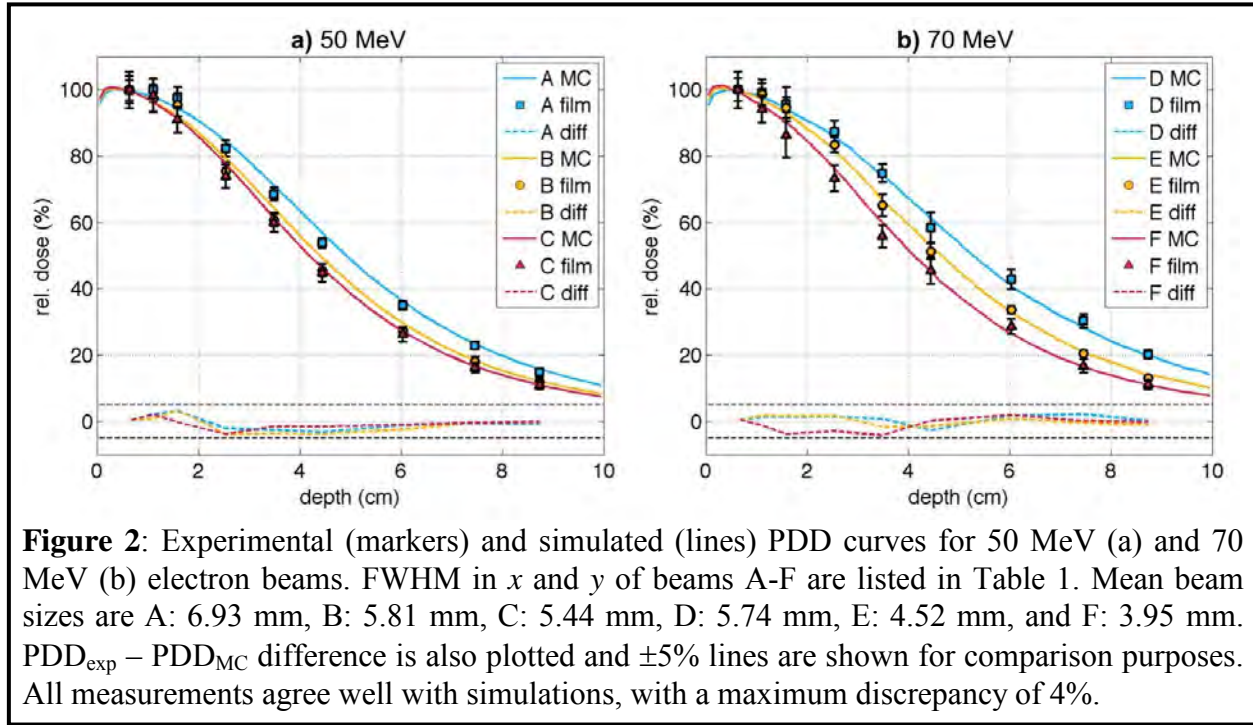
Table 1: Beam parameters, measured and simulated doses at 0.64 cm depth.

| Beam energy		50 MeV			70 MeV		
Nominal size (mm)		**5**	**3**	**2**	**5**	**3**	**1**
Beam label		**A**	**B**	**C**	**D**	**E**	**F**
FWHM film @ 0.64 cm depth	*x* (mm)	7.31	5.80	5.45	4.47	4.43	4.00
	y (mm)	6.55	5.82	5.43	7.01	4.60	3.89
	mean (mm)	6.93	5.81	5.44	5.74	4.52	3.95
FWHM exit window	*x* (mm)	5.81	4.04	3.53	3.25	3.20	2.52
	y (mm)	4.80	4.06	3.51	6.12	3.42	2.33
Number of pulses with 30 pC		40	20	10	40	20	3
Measured dose (Gy)		2.87	3.03	1.20	1.79	6.29	1.08
Simulated dose (Gy)		4.06	2.73	1.54	6.23	4.67	0.95
Difference $(D_{MC}-D_{film})/D_{film}$		42%	-10%	28%	248%	-26%	-12%

3. Results

3.1. Comparison of experimental measurements and Monte Carlo simulations

The experimental and simulated PDD curves for all measured beam sizes of both energies are shown in Figure 2. The PDD$_{exp}$-PDD$_{MC}$ difference curves in Figure 2 demonstrate a good agreement between the experimental and simulation data with the largest discrepancy of 4%.

Figure 2: Experimental (markers) and simulated (lines) PDD curves for 50 MeV (a) and 70 MeV (b) electron beams. FWHM in *x* and *y* of beams A-F are listed in Table 1. Mean beam sizes are A: 6.93 mm, B: 5.81 mm, C: 5.44 mm, D: 5.74 mm, E: 4.52 mm, and F: 3.95 mm. PDD$_{exp}$ – PDD$_{MC}$ difference is also plotted and ±5% lines are shown for comparison purposes. All measurements agree well with simulations, with a maximum discrepancy of 4%.

Relative beam profiles of experimental D$_{exp}$ and simulated D$_{MC}$ relative doses for all 50 and 70 MeV beams at four depths ranging from 6.4 to 74.6 mm along both major axes are shown in Figures 3 and 4, respectively. Additionally, the dose difference D$_{exp}$-D$_{MC}$ is plotted. The results in Figure 3 show that the dose difference was within 5% for all 50 MeV measured points. Figure 4 demonstrates that the largest 70 MeV beam (beam D) was noticeably skewed in the *y* direction from clipping by the exit window, observed as profile dose differences up to 11%. The skewness effect diminished with increasing depth and it was unnoticeable at depth of 74.6 mm. With the exception of beam D profile in *y* direction, all 70 MeV experimental and simulated points were within 5%.
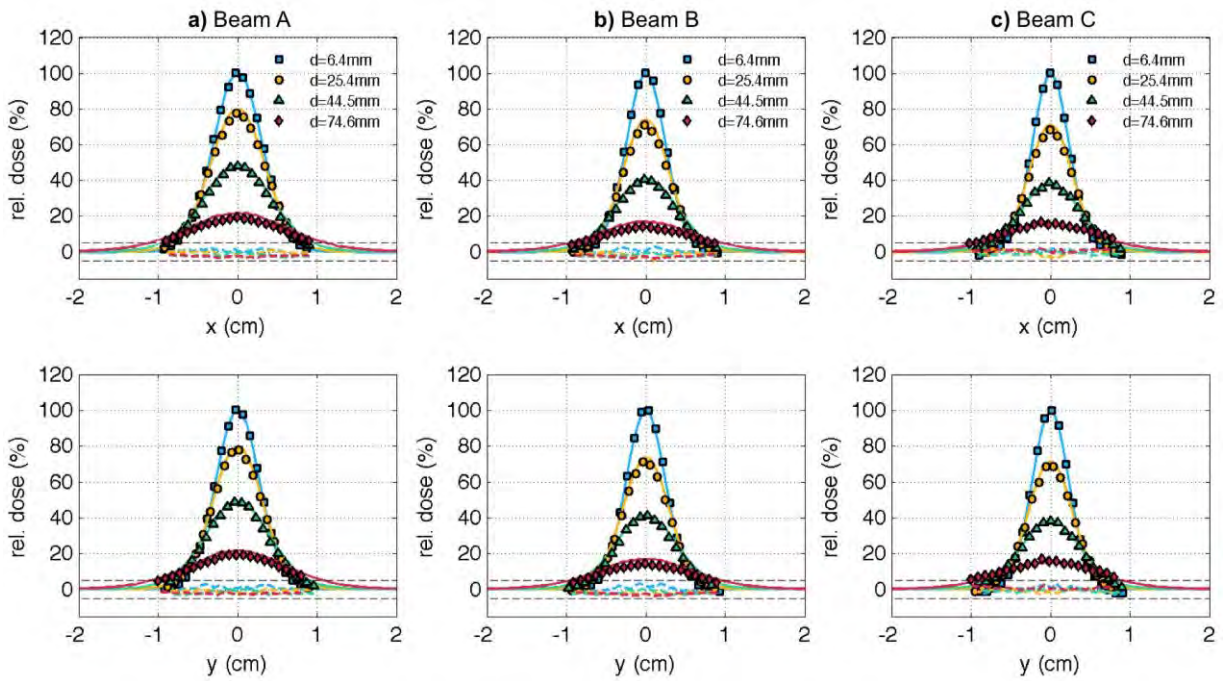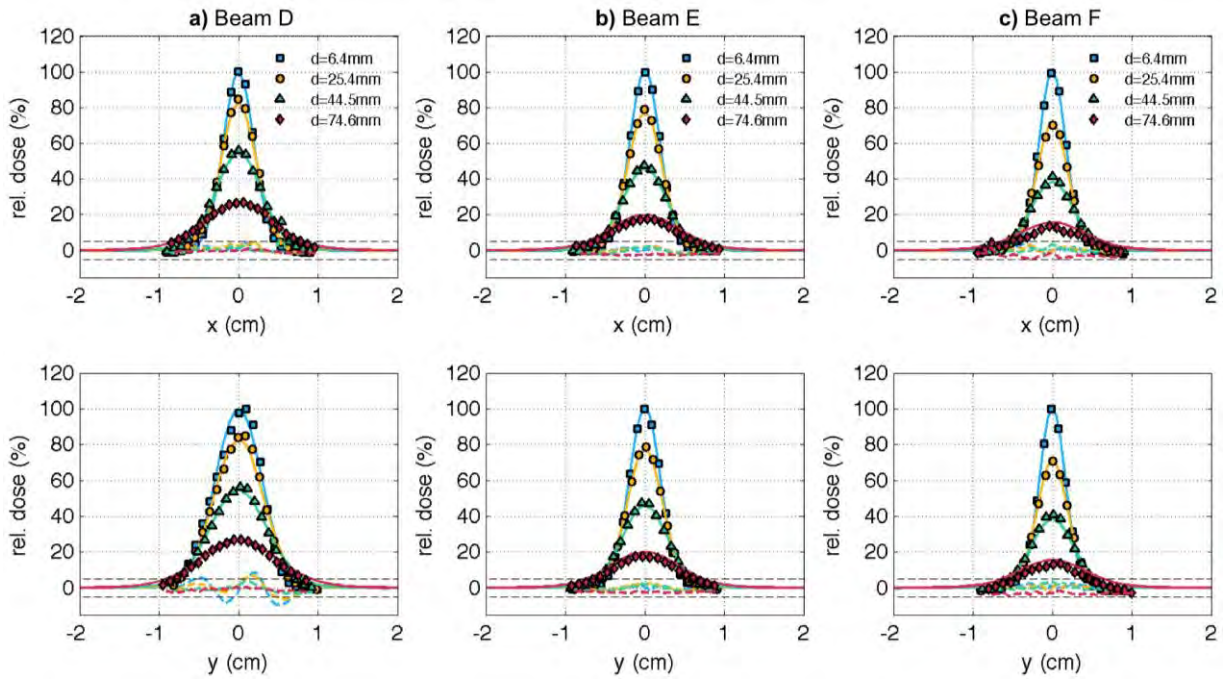
Figure 3: Experimental (markers), simulated (solid lines) and difference (dashed) profiles for the three 50 MeV beams (A: 6.93 mm, B: 5.81 mm, C: 5.44 mm) plotted at four depths. The ±5% lines are shown for comparison purposes. All difference profiles fall between these lines.

3.2. VHEE beam spread due to the exit window, air, and uncertainty in beam energy and beam angular spread

As mentioned above, the beam size at the accelerator exit window was back-calculated based on simulation data presented in Figure 5a. The relationship between input beam width and beam width at the phantom was found to be non-linear and highly energy dependent. The minimum beam size at the first film for an infinitesimally small input beam was calculated to be 4.0 mm and 3.0 mm for the 50 MeV and 70 MeV beams, respectively.

Figure 4: Experimental (markers), simulated (solid lines), and difference (dashed) profiles for the three 70 MeV beams (D: 5.74 mm, E: 4.52 mm, and F: 2.40 mm) plotted at four depths. The ±5% lines are shown for comparison purposes. All difference profiles fall between these lines, except for Beam D (*y* direction) that shows skewing of the profiles indicating clipping of the beam by the exit window in that dimension.

Figure 5b summarizes the effects of beam energy and energy spread on central-axis depth dose curves of the largest 50 and 70 MeV beams. While the maximum difference in dose due to energy measurement uncertainty was 1.5% for the 50 and 70 MeV beam, energy spread of 0.25% FWHM had a negligible effect on central axis depth dose. The effect of the possible 0.286° beam angular spread resulted in maximum dose difference of 3.0% and 3.8% for the 50 and 70 MeV beam, respectively.
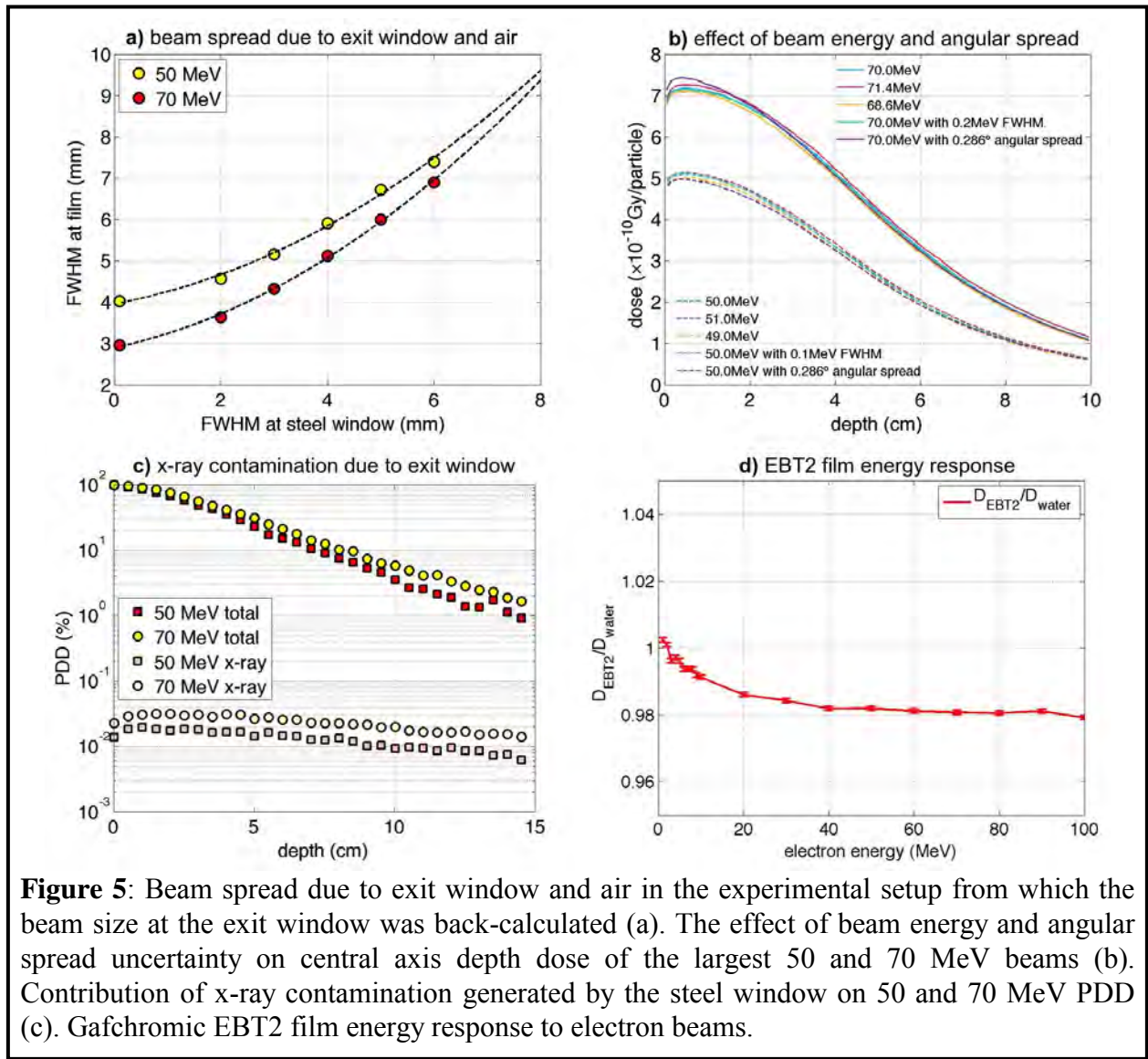
Figure 5: Beam spread due to exit window and air in the experimental setup from which the beam size at the exit window was back-calculated (a). The effect of beam energy and angular spread uncertainty on central axis depth dose of the largest 50 and 70 MeV beams (b). Contribution of x-ray contamination generated by the steel window on 50 and 70 MeV PDD (c). Gafchromic EBT2 film energy response to electron beams.

3.3. Monte Carlo modeling of x-ray contamination due to exit window

The effect of x-ray contamination of the electron beam due to the presence of the steel exit window for 50 and 70 MeV beams is presented in Figure 5c. The contribution of x-ray dose to the total central-axis dose on the surface was approximately $1\times10^{-2}\%$ and $2\times10^{-2}\%$ of the maximum dose for the 50 MeV and 70 MeV electron beam, respectively. Due to the faster attenuation of the electron beam, the relative x-ray dose contribution increased with depth. At 10 cm depth, the ratio of x-ray dose to total dose increased to 0.26% and 0.34% for the 50 MeV and 70 MeV beam, respectively. X-ray contamination was higher for the 70 MeV beam compared to

the 50 MeV beam due to the increasing bremsstrahlung cross-section with increasing electron beam energy.

3.4. EBT2 film energy response to electrons

The simulated energy response of EBT2 films for 1-100 MeV electrons plotted in Figure 5d suggests that Gafchromic EBT2 films have a flat <2.5% energy response in this energy range.

4. Discussion

4.1. Comparison of experimental and simulation data

The PDD curves in Figure 2 show good agreement between simulation and experimental data for both energies. Central axis PDD at 8 cm depth ranged from 14% to 19% for the 5.44-6.93 mm 50 MeV beams and it ranged from 14% to 24% for the 3.95-5.74 mm 70 MeV beams. Additionally, beam profiles presented in Figure 3 and 4 demonstrate how VHEE beam size increases with increasing depth.

The accuracy of MC simulations of the experimental setup was limited by a number of parameters that may have contributed to the observed differences with measurements. First, the beam size at the exit window was not known and was back-calculated from the measurement of the first film. Second, zero beam angular spread was assumed in the simulations. In the experimental setup, however, the beams were kept focused using a set of quadrupole magnets and as a result, beam angular spread was possibly non-zero. Finally, beam energy spread could not be controlled easily and it was approximately 2%. The effect of beam angular spread and energy spread on the PDD of the largest beam for both energies were presented and briefly discussed. Despite the uncertainties, agreement between Monte Carlo simulations and experiments was good. In future experiments, we plan to measure the beam size at the exit window, the beam angular spread, and the electron beam energy more accurately.

4.2. Absolute dosimetry

The maximum measured film doses on the first film placed at 0.64 cm depth were compared to MC simulated doses. The results are summarized in Table 1. Apart from the largest 70 MeV beam, MC doses differed from film doses by -26% to 42%. Large MC dose overestimation of 248% was found for the largest 70 MeV beam. This can be explained by the skewed beam profile that could not be accurately simulated, as well as the fact that the beam size in y direction exceeded the size of the exit widow (Table 1). We assume that beam D was not well centered on the exit window and clipped on one side as a result, which caused a significant charge loss.

MC simulated doses assumed Gaussian beams with a constant shape and stable charge during all irradiation pulses. However, such low beam charge could only be measured with 10% accuracy. Additionally, the charge could not be measured in real time and charge drifts due to the gun RF phase and laser power drift could be a possible source of absolute dose differences. Absolute dose differences could be further attributed to the fact that small apertures were used on the accelerating structures, which might have also scraped some charge. In summary, due to the current beam diagnostics and experimental setup, absolute dose differences up to 50% were expected.

5. Conclusions

We have performed a comparison of experimental homogeneous phantom dose measurements and EGSnrc Monte Carlo simulation of electron beams for energies of 50-70 MeV. Our experimental electron beam relative measurements at 50 and 70 MeV show good agreement with Monte Carlo results. Next steps will include experimentally validating MC dose calculations in the presence of heterogeneous phantoms. This will confirm that the physics of VHEE interactions with matter is sufficiently well understood to be accurately modeled by MC methods, allowing us to use them for the design and planning of future high-energy electron radiation

therapy systems. The MC model of the VHEE beam line will be used to calculate dose to samples in our future *in vitro* and *in vivo* studies of VHEE tumor and normal tissue radiobiology.

ACKNOWLEDGEMENTS

References:

1.   Khan FM, Stathakis S. The Physics of Radiation Therapy. Medical Physics. 2010;37(3):1374-5.

2.   Griep C, Davelaar J, Scholten AN, Chin A, Leer JWH. Electron-beam therapy is not inferior to superficial x-ray therapy in the treatment of skin carcinoma. International Journal of Radiation Oncology Biology Physics. 1995;32(5).

3.   Hoppe RT. Mycosis fungoides: radiation therapy. Dermatologic Therapy. 2003;16(4):347-54.

4.   DesRosiers C, Moskvin V, Bielajew AF, Papiez L. 150-250 MeV electron beams in radiation therapy. Physics in Medicine and Biology. 2000;45(7):1781-805.

5.   Papiez L, DesRosiers C, Moskvin V. Very high energy electrons (50-250 MeV) and radiation therapy. Technology in cancer research & treatment. 2002;1(2):105-10.

6.   Yeboah C, Sandison GA, Moskvin V. Optimization of intensity-modulated very high energy (50-250 MeV) electron therapy. Physics in Medicine and Biology. 2002;47(8):1285-301.

7.   Yeboah C, Sandison GA. Optimized treatment planning for prostate cancer comparing IMPT, VHEET and 15 MV IMXT. Physics in Medicine and Biology. 2002;47(13):2247-61.

8.   Moskvin V, Salvat F, Stewart DK, DesRosiers CM. PENELOPE Monte Carlo engine for treatment planning in radiation therapy with Very High Energy Electrons (VHEE) of 150-250 MeV. 2010 IEEE Nuclear Science Symposium and Medical Imaging Conference (2010 NSS/MIC). 2010.

9.   Baro J, Sempau J, Fernandezvarea JM, Salvat F. PENELOPE - An algorithm for Monte-Carlo simulation of the penetration and energy-loss of electrons and positrons in matter. Nuclear Instruments & Methods in Physics Research Section B-Beam Interactions with Materials and Atoms. 1995;100(1):31-46.

10.   Chetty IJ, Moran JM, Nurushev TS, McShan DL, Fraass BA, Wilderman SJ, et al. Experimental validation of the DPM Monte Carlo code using minimally scattered electron beams in heterogeneous media. Physics in Medicine and Biology. 2002;47(11):1837-51.

11.   Chetty IJ, Moran JM, McShan DL, Fraass BA, Wilderman SJ, Bielajew AF. Benchmarking of the Dose Planning Method (DPM) Monte Carlo code using electron beams from a racetrack microtron. Medical Physics. 2002;29(6):1035-41.

12.   Brahme A, Kraepelien T, Svensson H. Electron and photon beams from a 50 MeV racetrack microtron. Acta Radiologica Oncology. 1980;19(4):305-19.

13.   Kawrakow I, Rogers DWO. The EGSnrc code system: Monte Carlo simulation of electron and photon transport. 2006.

14.   Dunning M, Adolphsen C, Chu TS, Colby E, Gilevich S, Hast C, et al. Status and upgrade of NLCTA for studies of advanced beam acceleration, dynamics and manipulations. energy. 2011;100(1):T2.

15.   Rogers DWO, Faddegon BA, Ding GX, Ma CM, We J, Mackie TR. BEAM - A Monte-Carlo code to simulate radiotherapy treatment units. Medical Physics. 1995;22(5):503-24.

16.   Walters BRB, Kawrakow I, Rogers DWO. DOSXYZnrc users manual. NRCC; 2007.

17.   Arjomandy B, Tailor R, Anand A, Sahoo N, Gillin M, Prado K, et al. Energy dependence and dose response of Gafchromic EBT2 film over a wide range of photon, electron, and proton beam energies. Medical Physics. 2010;37(5):1942-7.

18.   Sutherland JGH, Rogers DWO. Monte Carlo calculated absorbed-dose energy dependence of EBT and EBT2 film. Medical Physics. 2010;37(3):1110-6.

19.   Karsch L, Beyreuther E, Burris-Mog T, Kraft S, Richter C, Zeil K, et al. Dose rate dependence for different dosimeters and detectors: TLD, OSL, EBT films, and diamond detectors. Medical Physics. 2012;39(5):2447-55.